Prediction of fabrication distortions in step and flash imprint lithography templates

C. J. Martin, R. L. Engelstad,[a] and E. G. Lovell
Computational Mechanics Center, University of Wisconsin, 1513 University Ave., Madison, Wisconsin 53706

D. J. Resnick
Motorola Labs, Physical Sciences Research Laboratories, Tempe, Arizona 85284

E. J. Weisbrod
Motorola, DigitalDNA™ Laboratories, Tempe, Arizona 85284

(Received 28 May 2002; accepted 23 September 2002)

Step and flash imprint lithography (SFIL) is an alternative approach for printing sub-100 nm features that relies on chemical and mechanical techniques to transfer patterns. The imprint process requires no projection optics and is performed at room temperature with low imprint pressures to reduce thermal and mechanical template distortions. Because imprint lithographies are 1× pattern transfer processes that preclude magnification corrections, the minimization of template distortions during fabrication and imprinting is critical. The processes and materials used in the fabrication of SFIL templates are similar to those used in the manufacturing of optical masks. The various process steps have been simulated using finite element techniques in order to predict the resulting pattern distortions. Two proposed template fabrication schemes were modeled, the resulting pattern distortions compared, and the error sources were quantified. © *2002 American Vacuum Society.*
[DOI: 10.1116/1.1521743]

I. INTRODUCTION

Step and flash imprint lithography (SFIL) is a patterning technique with the potential of producing sub-100 nm resolution while not requiring expensive projection optics or advanced illumination sources.[1] In imprint lithography, the topography of a template defines the patterns created on a substrate. Because imprint lithography is a 1× pattern transfer process, the production of high quality templates and the minimization of pattern distortions are critical. SFIL templates can be fabricated using standard phase-shift mask manufacturing techniques and materials,[2] and one potential source of pattern distortions is the template fabrication process. Therefore, it is important to understand and quantify the sources of pattern distortions during template production. To this end, finite element analysis has been used to numerically simulate two proposed fabrication process flows: a chrome-on-glass template and an indium tin oxide (ITO)/oxide template that incorporates a conductive ITO layer to facilitate inspection.[3] These simulations include each process step and track the changes in in-plane distortion (IPD) and out-of-plane distortion (OPD) between e-beam patterning and the final imprint topography for the two template formats.

II. IMPRINT TEMPLATES

Currently, imprint template fabrication schemes start with a standard 6 in.×6 in.×0.25 in. (152.4 mm×152.4 mm ×6.35 mm) quartz mask blank.[2] After the etching of the template topologies on the blank, the individual templates are cut from the plate. The current template form factor is 1.0 in.×1.0 in. (25.4 mm×25.4 mm). For these analyses, it was assumed that a 4×4 array of templates was printed on each mask blank as illustrated in Fig. 1. This layout allowed for the evaluation of pattern distortions with respect to location on the blank. The chrome-on-glass template uses a thin chrome layer (<20 nm) as a hard mask for the transfer of the image to the quartz. In this process, as illustrated in Fig. 2, the thin chrome and resist layers are deposited on the quartz substrate (Steps 1 and 2). The chrome layer had a stress of 100 MPa and a thickness of 20 nm, and the resist stress and thickness were 10 MPa and 150 nm, respectively. A summary of the process parameters used in the simulations is given in Table I. The resist is then patterned with an e beam, and the exposed resist is stripped away (Step 3). After the exposed chrome is removed (Step 4), the quartz is etched (Step 5) creating the pattern topography on the mask. Typical etch depths into the quartz are 100 nm.[3] The remaining resist and chrome are then stripped away (Step 6), and the 1.0 in.×1.0 in. templates are cut from the blank (Step 7).

The ITO/oxide template scheme is being developed to overcome some of the inspection limitations of the previously described process. Because features in chrome-on-glass templates are directly patterned in the quartz, electron beam and optical inspections are problematic. The ITO/oxide template includes a transparent, conducting ITO layer on the surface that facilitates inspection. The process used to fabricate this type of template is illustrated in Fig. 3. An ITO film is deposited directly on the glass (Step 1) followed by a silicon dioxide (SiO_2) layer (Step 2). The ITO film in these analyses was assigned a thickness of 60 nm and a stress of 200 MPa while the SiO_2 layer had a thickness of 100 nm and a stress of −50 MPa (see Table I). Following this, the resist is deposited (Step 3), patterned with an e beam and devel-

[a]Electronic mail: engelsta@engr.wisc.edu

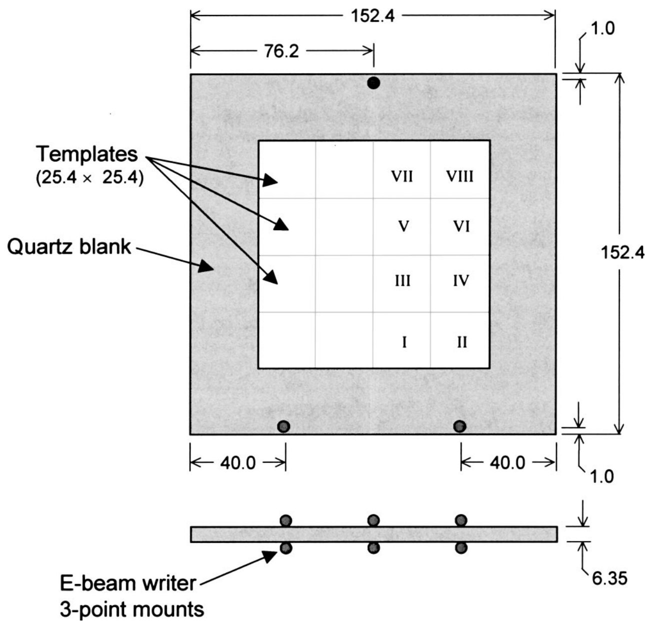

FIG. 1. Layout of the individual templates of the quartz blank and locations of the e-beam writer three-point mount supports. Dimensions in mm.

TABLE I. Component thicknesses and stress levels for the chrome-on-glass and ITO/oxide template fabrication processes.

Chrome-on-glass template	Thickness	Stress
Quartz substrate	6.35 mm	0 MPa
Chrome	20 nm	100 MPa
Resist	150 nm	10 MPa
ITO/oxide template	**Thickness**	**Stress**
Quartz substrate	6.35 mm	0 MPa
Indium tin oxide	60 nm	200 MPa
Silicon dioxide	100 nm	−50 MPa
Resist	150 nm	10 MPa

oped (Step 4). The template topography is then transferred to the SiO_2 layer with the resist serving as the etch mask (Step 5). The ITO remains on the mask and provides contrast for inspection. Finally, the resist is stripped (Step 6), and the templates are cut (Step 7).

III. FINITE ELEMENT SIMULATIONS

Numerical simulations of each fabrication process were performed using the commercial finite element code ANSYS®, and the IPD and OPD results at the individual steps were recorded. The deposition and etching of the various film layers as well as the cutting of the templates from the mask blank were modeled using the element birth/death option in ANSYS®. Pattern transfer distortions are determined from the change in local IPD of each template from e-beam patterning to the final topography of the 1.0 in.×1.0 in. format template. The local distortions are computed with respect to a reference point on each individual template—the upper left corner in this work. Because each template will be separate and aligned independently for imprinting, the overall distortions of the quartz blank during patterning are irrelevant, and only changes in IPD within an individual template are of interest. Two pattern densities, 20% and 50%, were assumed for the ITO/oxide template, and the patterns were considered to be uniform and isotropic. The chrome-on-glass template distortions are pattern independent because the final patterned templates consist entirely of stress-free glass.

The fabrication-induced image placement errors predicted in this work can primarily be attributed to two sources: (1) the deposition and removal of the stressed film layers as described in the process flows and (2) the mounting in the e-beam writer and imprint tool. Because the templates are fabricated using conventional photomask blanks, they can be patterned using the standard three-point mount in the e-beam writer. The locations of the three-point mount supports are shown in the schematic of the blank (Fig. 1). The mask blank

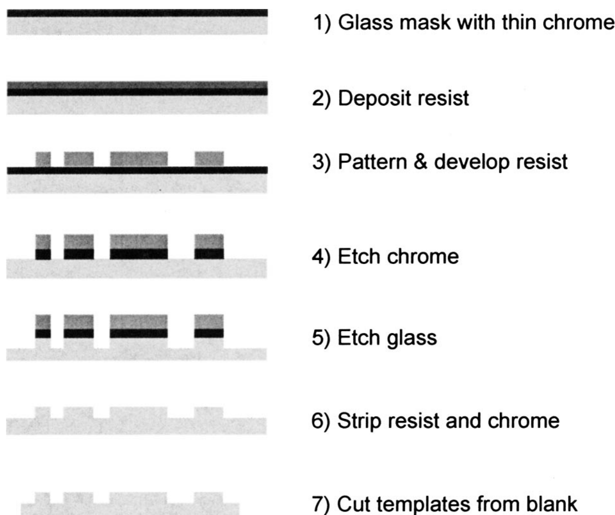

FIG. 2. Fabrication process flow for the chrome-on-glass template.

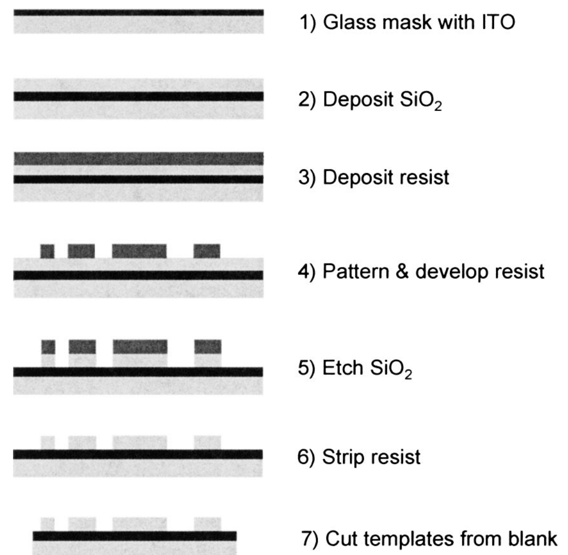

FIG. 3. Fabrication process flow for the ITO/oxide template.

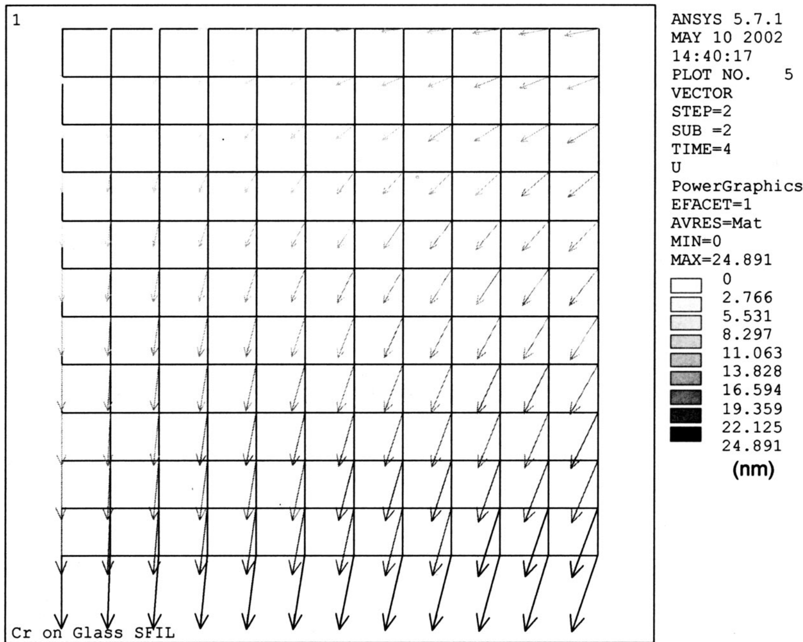

FIG. 4. Pattern transfer IPD vectors for template V of the chrome-on-glass format. The maximum IPD is 24.9 nm.

is held horizontally in the e-beam tool, and in the finite element simulations the mask was constrained normal to the surface at these points, and a gravitational load was included. Additionally, the constraints allowed for free in-plane motion of the mask blank. Because the individual template distortions were measured with respect to the upper left corner of each individual template, the reported template distortion data are independent of the in-plane constraint point. The support of the templates in the imprint tool is less well defined, but the smaller 1.0 in.×1.0 in. format of the templates significantly reduces the effects of mounting conditions and gravitational sag. Analyses assuming different template support conditions indicated that gravity loads contributed less than 1 nm to both template OPD and IPD. Therefore, gravitational forces were not included in computing the final template distortions, and the models were constrained only to prevent rigid body motions neglecting imprint tool mounting distortions.

IV. RESULTS

The finite element simulations were performed for both the chrome-on-glass and ITO/oxide template formats. Of primary interest was the pattern transfer IPD on each of the individual templates. The template layout and three-point mount orientation provide horizontal symmetry across the

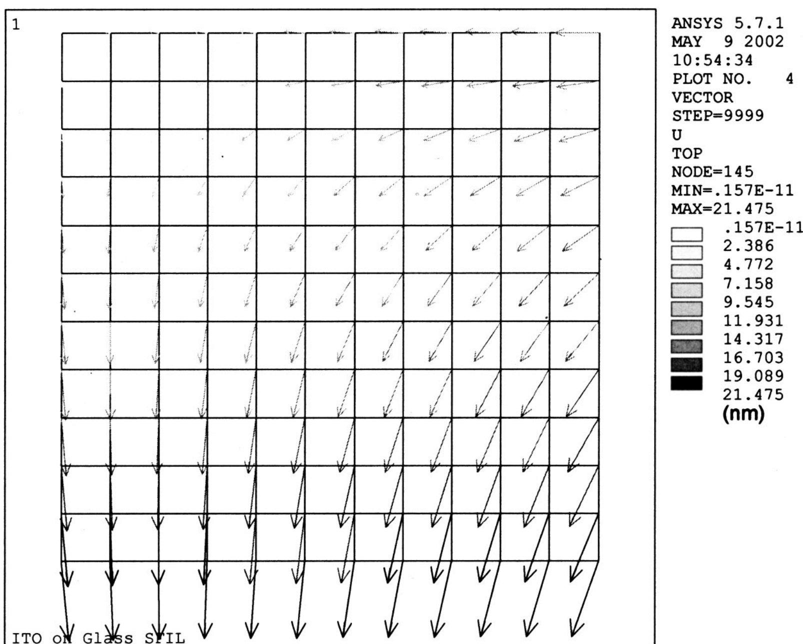

FIG. 5. Pattern transfer IPD vectors for template V of the ITO/oxide format. The maximum IPD is 21.5 nm.

TABLE II. Maximum pattern transfer IPD for the various template locations as defined in Fig. 1 for the chrome-on-glass and ITO/oxide template formats. Additionally, predicted IPD for an uncoated mask blank are included.

Template No.	Chrome-on-glass Pattern independent IPD (nm)	ITO/oxide 50% pattern IPD (nm)	ITO/oxide 20% pattern IPD (nm)	Glass only Grav. effects IPD (nm)
I	18.2	16.7	16.5	17.8
II	17.8	16.0	15.8	17.1
III	23.1	21.1	20.9	22.7
IV	22.5	20.2	19.8	22.0
V	24.9	21.5	21.2	24.5
VI	23.8	21.3	20.9	23.3
VII	24.7	19.8	19.4	24.4
VIII	21.3	20.2	20.0	20.7

model, reducing the computational time and also the number of templates to be tracked. For reference, the eight unique templates were assigned numbers as indicated in Fig. 1. Template V was found to have the highest pattern transfer distortions for both formats studied. The maximum pattern transfer IPD on this template was 24.9 nm for the chrome-on-glass format (Fig. 4) and 21.5 nm for the ITO/oxide format (Fig. 5) with 50% pattern coverage. The patterning distortions presented in Figs. 4 and 5 are with respect to a reference point at the upper left corner of each template, and hence the IPD at this corner will be zero in all cases. Examination of the maximum pattern IPD of the remaining templates indicated a 25% variation across the mask blank. The results for each template are summarized in Table II. Template II had the minimum IPD in all cases, and for the ITO/oxide process, the 50% coverage case had slightly higher pattern transfer distortions than the 20% coverage case. The maximum difference due to pattern coverage was only 2%. OPD results were also examined to determine their potential impact on imprinting. The chrome-on-glass templates, being stress free in their final state, had zero OPD, and OPD for the ITO/oxide templates was less than 3 nm.

The predicted pattern transfer distortions were quite similar for the two processes as were the variations with template location on the mask. Further examination of the results indicated that a major source of the pattern transfer distortions was gravitational sag in the e-beam writer: the maximum OPD in the e-beam writer was 965 nm for the chrome-on-glass format and 967 nm for the ITO/oxide format. In order to isolate this effect, a simulation that predicted the distortions for a simple quartz glass blank was developed. This removed the effects of the deposition and removal of the various stressed films, isolating the distortions due to gravitational sag. The maximum predicted IPD in each template for the glass only case is also listed in Table II. The results for this case were quite similar to those of chrome-on-glass templates, and the inclusion of the chrome and resist layers adds less than 0.4 nm to the template distortions. The smaller pattern transfer distortions in the ITO/oxide templates were the result of the remaining stressed ITO layer on the final templates. This layer produced distortions in the individual 1.0 in.×1.0 in. templates that partially compensated for the gravitational sag IPD. Because the pattern transfer distortions were primarily due to sag in the e-beam writer and were relatively independent of pattern density, they could likely be compensated for. (Compensations for mask height variations, for which sag is a component, have been implemented in e-beam writers,[4] but the methods are generally proprietary which precludes evaluation here.) For imprint templates, this compensation would have to be performed during e-beam patterning, and would have to be applied to the pattern on each template rather than the overall mask blank.

To investigate the potential efficacy of pattern corrections,

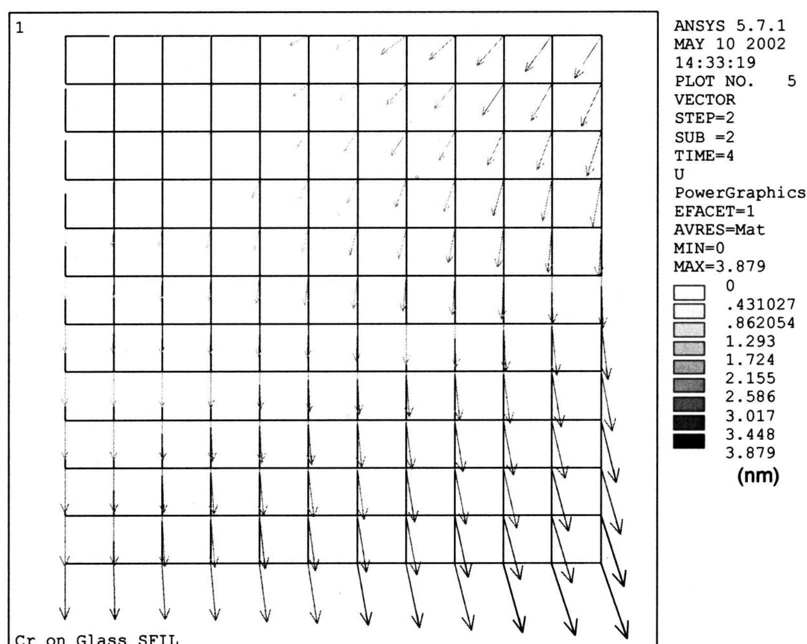

FIG. 6. Pattern transfer IPD vectors for template V of the chrome-on-glass format after application of uniform template magnification corrections. The maximum IPD is 3.9 nm.

simulated x and y magnification corrections across each template were applied to the results, and the maximum template IPD was reduced to 8.5 nm for the chrome-on-glass format. The same correction factors were used on all templates, and the values selected were not optimized. The corrected distortion vectors for Template V are shown in Fig. 6. The maximum pattern transfer IPD has been reduced from 24.9 to 3.9 nm with the correction used. This could be reduced further if corrections were developed independently for each template.

V. SUMMARY AND CONCLUSIONS

Finite element models have been developed to simulate the fabrication processes and predict the pattern transfer distortions of two candidate SFIL template formats. Pattern transfer IPD was found to be about 20 nm over the 1.0 in. $\times$1.0 in. templates and was slightly higher for the chrome-on-glass templates compared to the ITO/oxide format. In addition, the location of the template on the mask blank also affected pattern transfer IPD. There was approximately a 25% variation in the maximum IPD for each template format depending on the location of the template in the quartz blank. Further analysis indicated that most of the patterning errors could be attributed to gravitational sag in the e-beam writer, and that much of this could be reduced by including magnification corrections during e-beam patterning. Because of the thick substrates and relative small size of the templates, pattern density had little effect on final template IPD. These results do not include distortions that may be induced by mounting the imprint tool. Because SFIL is a 1$\times$ process, care must be taken to minimize all sources of distortions.

ACKNOWLEDGMENTS

This research has been funded in part by DARPA/ARL, International SEMATECH, and the Semiconductor Research Corporation (SRC). Computer support was provided by International SEMATECH, Intel, and Microsoft.

[1]T. Bailey, B. Smith, B. J. Choi, M. Colbrun, M. Meissl, and S. V. Sreenivasan, J. Vac. Sci. Technol. B **19**, 2806 (2001).
[2]M. Colbrun, T. Bailey, B. J. Choi, J. G. Ekerdt, S. V. Sreenivasan, and C. G. Willson, Solid State Technol. **44**, 67 (2001).
[3]D. Resnick, W. Dauksher, D. Mancini, K. Nordquist, E. Ainley, K. Gehoski, J. Baker, T. Bailey, B. Choi, S. Johnson, S. Sreenivasan, J. Ekerdt, and C. Willson, Proc. SPIE **4688** 205 (2002).
[4]H. Pearce-Percy, R. Prior, F. Abboud, A. Benveniste, L. Gasiorek, M. Lubin, and F. Raymond, J. Vac. Sci. Technol. B **12**, 3393 (1994).